KEK Preprint 94-188
DPNU-95-03
January 1995
H

A Profile and Flux Monitor for the Few GeV Neutron Beam at KEK

T. SASAKI, T. HASEGAWA, S. HIRATA, N. HORIKAWA, S. ISHIMOTO, T. IWATA, M. KAWABATA, Y.D. KIM, M.A. KOVASH, Y. MIYACHI, Y. MIZUNO, F. NAKAYAMA, H. OGAMI, A. OGAWA, S. SAWADA, T.-A. SHIBATA, K. TAMURA and J. TRICE

Submitted to Nucl. Instrum. Meth., A.

KEK Reports are available from:

Technical Information & Library
National Laboratory for High Energy Physics
1-1 Oho, Tsukuba-shi
Ibaraki-ken, 305
JAPAN

Phone: 0298-64-1171
Telex: 3652-534 (Domestic)
(0)3652-534 (International)
Fax: 0298-64-4604
Cable: KEK OHO
E-mail: LIBRARY@JPNKEKVX (Bitnet Address)
library@kekvax.kek.jp (Internet Address)

A profile and flux monitor for the few GeV neutron beam at KEK

T.Sasaki[1] * , T.Hasegawa[2], S.Hirata[3], N.Horikawa[1], S.Ishimoto[4] T.Iwata[1] † , M.Kawabata[3], Y.D.Kim[4], M.A.Kovash[5], Y.Miyachi[1], Y.Mizuno[3], F.Nakayama[2], H.Ogami[6], A.Ogawa[1], S.Sawada[7], T.-A.Shibata[5,6], K.Tamura[3], J. Trice[5]

[1] *Nagoya University, Furo-Cho, Chikusa-ku, Nagoya 464, Japan*
[2] *Miyazaki University, Gakuen-Kihanadai, Nishi-1, Miyazaki 889-21, Japan*
[3] *RCNP, Osaka University, Ibaraki, Osaka, 567, Japan*
[4] *KEK, Tsukuba, Ibaraki, 305, Japan*
[5] *University of Kentucky, Lexington, KY40506, USA*
[6] *Tokyo Institute of Technology, Megro, Tokyo,152, Japan*
[7] *Kyoto University, Sakyo, Kyoto, 606, Japan*

submitted to Nucl. Instrum.and Methods A

Abstract

We describe a neutron beam monitor in the few GeV region developed for an experiment of the n+p $\rightarrow$ d+γ differential cross section measurement at the KEK-PS. It was used to monitor the profile and the flux of the neutron beam. The detector is a 3-plane plastic scintillator hodoscope. We present the design and performance of the monitor. The detection efficiencies evaluated with various Monte Carlo simulation codes are compared to the results of the measurements.

1 Introduction

Plastic scintillators have been widely used to detect neutrons which appear in the final state of nuclear reactions [1]. However, the neutron detector which we present here is designed to monitor the profile (two-dimensional spatial distribution) and flux of a neutron beam at a few GeV, and is installed on the beam axis. Therefore, there was a novel point which has to be considered for the present work: the neutron interaction with the scintillator material at a few GeV is complicated, unlike at low and medium energy. The main complication is due to the generation of multiple pions in the hadron cascade. The hadron cascade therefore has to be carefully simulated when the monitor is designed. We used three different simulation codes (TATINA [2] ,GHEISHA [3] ,FLUKA [4]) to check the mutual consistency of the neutron detection efficiency and to optimize the scintillator thickness. We found that a rather consistent detection efficiency is obtained from the three simulations for a total neutron monitor thickness of 1 cm.

This means, however, that about 1% of the neutron beam interacts with the scintillator, resulting in rather high counting rates as the neutron flux is about 10^8 per spill. The spill time of the slow extraction beam at the KEK proton synchrotron is about 2 seconds. We investigated possible detection inefficiencies and distortions of the monitored beam profile using the actual neutron beam. The detection efficiency was measured in a neutron beam of known flux. We conclude that the profile and flux can be monitored with good precision using the neutron detector which is presented here.

*Present address: *Toyota Central Research & Development Labs., inc., Nagakute-cho, Aichi 480-11, Japan*

†email address: *iwata@kekvax.kek.jp*

2 The neutron beam line

A brief description of the neutron beam line is given in this section. The details have been reported elsewhere [5]. The neutron beam line was constructed at one of the extraction beam lines, P1, of the KEK 12-GeV proton synchrotron (KEK-PS). The setup of the neutron beam line is shown in Fig.1. Neutrons were produced by the proton-stripping reaction of a deuteron beam in a 6 cm thick beryllium target. The deuteron beam of 2 $\sim$ 6 GeV irradiating the beryllium target provided a nearly monoenergetic neutron beam in the energy range from of 1 $\sim$ 3 GeV. The neutrons passing through the sweeping magnet were collimated with two collimators made of lead. Both had a rectangular opening tapered along the beam axis; the size of the opening was 34x34mm^2 at the entrance of the first collimator, and 52x52mm^2 at the exit of the second. The neutron beam line was designed for an experiment (E235) to measure the differential cross section for the $n+p \rightarrow d+\gamma$ reaction, which was performed in April, 1993 [6]. Our neutron beam monitor was developed to monitor the flux and profile of the neutron beam in this experiment. The experimental setup is shown in Fig.2. The neutron beam monitor was installed at the most downstream end of the setup, and was used to continuously monitor the neutron beam.

3 Design and construction of the neutron beam monitor

The neutron beam monitor consisted of three planar arrays of plastic scintillator hodoscopes, as shown in Fig.3.

There were two reasons why the monitor was constructed as segmented hodoscopes. One is to allow measurements of the beam profile, the other is to maintain a relatively low counting rate in each photomultiplier tube. The sizes of the planes are: first plane- 380mm^W $\times$ 210mm^H , second plane- 200mm^W $\times$ 200mm^H and third plane- 260mm^W $\times$ 204mm^H . The first and third planes were made of horizontal scintillator bars 15mm wide and 2mm thick. The second plane was divided into the upper and the lower halves, each of them was made of vertical scintillator bars which are 20mm wide and 10mm thick. This configuration provided hodoscopes with 16, 10 (each half) and 13 channels for the first, second and third planes, respectively. The scintillation light collected from one side of each bar was fed to a HAMAMATSU H3165B 1/2" diameter photomultiplier tube equipped with a booster voltage supply for the high counting rate. The first plane was used to veto charged particles. Neutrons passing through the first plane and interacting in the second plane with its constituent nuclei (hydrogen and carbon) produce charged secondaries. They are then detected in the second and the third planes. Based on the nuclear interaction length of 78.8 cm in the plastic scintillator [13], the interaction probability of a neutron in the second plane is expected to be 1.26 %.

4 Electronics

The electronics diagram of the neutron beam monitor is shown in fig.4. The analogue signal of each photomultiplier in the second plane was divided into two lines; one was led to a discriminator and another to a CAMAC ADC to provide a pulse-height spectrum. The analogue signals from the other planes were sent only to discriminators. The discriminator outputs from each plane were sent to a logical OR module. The output signals of the OR modules were called F1, F2 and F3 for the first, the second and the third plane, respectively. These were were fed into coincidence modules to form the trigger signals. We used two types of trigger logic, "neutral logic" and "charged logic" as follows:

neutral logic: $\overline{\mathrm{CB}} \cdot \overline{\mathrm{F1}} \cdot \mathrm{F2} \cdot \mathrm{F3}$

charged logic: $\mathrm{F1} \cdot \mathrm{F2} \cdot \mathrm{F3}$

where CB (Charged Beam) is the signal from a thin plastic scintillation counter installed several meters upstream of the experimental setup. Signals from CB were used to eliminate most of the charged particles contaminating the neutron beam (see fig.2). The "neutral logic" trigger was used to select the neutrons which passed through the first plane and initiated nuclear interactions in the second plane with charged secondaries entering the third plane. The "charged logic" was used to trigger the charged particles passing through the neutron beam monitor. This trigger was used to measure the contamination of charged particles in the beam. All the discriminator outputs were lead to CAMAC coincidence register to provide hit pattern of the hodoscopes.

5 Beam profile measurements

The second and the third planes of the neutron beam monitor provided us with horizontal and vertical profiles, respectively, of the neutron beam. For this measurement the neutron beam monitor was installed 9.85m downstream of the Be target. This was the position of the liquid hydrogen target during the E235 experiment. The solid angle for the neutrons determined by the collimators was 50 μsr. The distance from the Be target and the collimator solid angle determined the beam profile at the neutron monitor. A GEANT simulation was done to estimate the profile of the neutron beam at the monitor position. The expected profile was the square $7.0 \times 7.0\ cm^2$, which was consistent with the measured profile using the "neutral logic", as shown in Fig.5. Measurements of the beam profile at the position of the liquid hydrogen target were performed several times during the construction of the neutron beam line.

When the profile of the charged contamination was required, data were collected with the "charged logic" trigger.

6 Data Analyses

6.1 Time structure of the beam spills

Before the corrections for dead time and accidental coincidences are made, it is necessary to define and measure the effective spill length. The KEK-PS provides a slow extracted beam with a beam spill length of $1.5 \sim 2.0$ sec in each acceleration cycle of 4 sec. The beam intensity during the spill had a modulation of the time scale of microseconds, which can affect the dead time correction of the neutron beam monitor. Such a time structure produces a shorter effective spill length than the total spill length given above. The effective spill length, T_{eff}, can be derived from the counting rate of the accidental coincidence $F2_{acc} = F2 \cdot F2_{del}$ where $F2_{del}$ is the 100ns delayed signal of F2:

$$T_{eff} = \frac{[F2]^2 \cdot W}{[F2_{acc}]} \tag{1}$$

The symbol "[ ]" denotes the total counts in a spill. W is the time width of the electronic components for chance coincidences: we found W to be 8ns, which is about double the width of the F2 pulse. Under the typical beam condition, T_{eff} was ~ 0.4 sec/spill.

6.2 Counting rate Corrections

Two kinds of corrections were applied to the measured counting rates: (1) the dead time correction, and (2) the accidental coincidence correction.

The dead time correction is given by

$$n = m \frac{T_{eff}}{T_{eff} - m\tau} \tag{2}$$

where n and m denote "true" and "measured" counts in a spill, and τ is the overall dead time. Since the neutron beam monitor consisted of scintillators and photomultipliers with a fast time response, only the dead time of the electronics was significant. The dead time of the electronics is determined by the width of the signal and the period during which the electronics does not function after each signal. The latter was $5 \sim 10$ns for the electronics we used in the measurement. The typical counting rates after the dead time correction are shown in Table 1.

To the measured coincidence counting rates, a correction for accidental coincidences was applied. In particular, for the neutron beam it often occurred that a hit was detected in only one of the three planes F1, F2 and F3. This background leads to a significant accidental coincidence probability. The correction was made in the following way, for example, for F2 and F3. Taking only F2 and F3 into account, the events are divided into the following four types :

Ev1–a hit in F2 without a hit in F3
Ev2–a hit in F3 without a hit in F2
Ev3–true coincidence of F2 and F3
Ev4–accidental coincidence of F2 and F3

There is a relation between the counting rates of these types of event :

$$[\mathrm{Ev4}] = \frac{([\mathrm{Ev1}] + [\mathrm{Ev4}])([\mathrm{Ev2}] + [\mathrm{Ev4}]) \cdot \mathrm{W}_{\mathrm{F2 \cdot F3}}}{\mathrm{T}_{\mathrm{eff}}} \quad (3)$$

where $\mathrm{W}_{\mathrm{F2 \cdot F3}}$ denotes the period for chance coincidence between F2 and F3. With the expressions

$$[\mathrm{Ev1}] = [\mathrm{F2}] - [\mathrm{F2} \cdot \mathrm{F3}]$$
$$[\mathrm{Ev2}] = [\mathrm{F3}] - [\mathrm{F2} \cdot \mathrm{F3}]$$

and replacing [Ev4] by the accidental coincidence rate $[\mathrm{N}_{\mathrm{acc}}]$, eq(3) is expressed as

$$[\mathrm{N}_{\mathrm{acc}}] = \frac{([\mathrm{F2}] - [\mathrm{F2} \cdot \mathrm{F3}] + [\mathrm{N}_{\mathrm{acc}}])([\mathrm{F3}] - [\mathrm{F2} \cdot \mathrm{F3}] + [\mathrm{N}_{\mathrm{acc}}]) \cdot \mathrm{W}_{\mathrm{F2 \cdot F3}}}{\mathrm{T}_{\mathrm{eff}}} \quad (4).$$

Then the corrected coincidence rate of $[\mathrm{F2} \cdot \mathrm{F3}]$ is given by

$$[\mathrm{F2} \cdot \mathrm{F3}]_{\mathrm{corr}} = [\mathrm{F2} \cdot \mathrm{F3}] - [\mathrm{N}_{\mathrm{acc}}] \quad (5).$$

The corrected coincidence rates of various triggers obtained in a similar way are summarized in Table 2.

****** Table 1 *******

****** Table 2 *******

7 Detection efficiency

7.1 Evaluations from the deuteron beam intensity

7.1.1 Measurements of the deuteron beam intensity

The deuteron beam intensity was measured with the Secondary Emission Chamber (SEC) located upstream of the neutron production target. The SEC is an ionization chamber using aluminum foils as a radiator. When the deuteron beam passes through the foils, secondary electrons are emitted and detected in the SEC.

The SEC was calibrated using the foil activation method [7] , in which the 1368.5 KeV $\gamma-$ray from ^{24}Na produced in the reaction ^{27}Al(d, 3dn)^{24}Na was detected by a Ge detector. The cross section for this reaction has been measured at 2.33 GeV ($\sigma = 15.25 \pm 1.5$ mb) [8] and at 7.3GeV ($\sigma = 14.7 \pm 1.2$ mb) [9] . Assuming the cross section is constant (15 ± 1.5 mb) from 2 to 6 GeV, the integrated deuteron flux was calculated from the γ-ray yield and compared with the SEC integrated charge. The SEC output was thus calibrated to provide integrated deuteron fluxes to $\sim 11\%$ accuracy. The sources of error in the intensity measurement were uncertainty of the detection efficiency of the Ge detector ($\sim 5\%$), the statistical error of $\gamma-$ray detection ($\sim 1\%$), the uncertainty in the thickness of the aluminum radiator foil ($< 1\%$) and uncertainty in the reaction cross section ($\sim 10\%$).

7.1.2 The Neutron Production

In order to estimate the neutron flux from the measured deuteron beam intensity, one should give the production efficiency. The differential cross sections for $d + ^9Be \rightarrow n + X$ at 0° in the several GeV region are reported at the neutron momenta 1.35GeV/c [10], 1.77Gev/c [11], and 2.90GeV/c [12]. Fitting the data with a linear function of the neutron momentum P_n (in GeV/c), the differential cross section (in barn/sr.) is expressed as

$$\frac{d\sigma}{d\Omega}(\Theta = 0°) \simeq 24 \cdot P_n - 10 \tag{6}$$

.

The neutron production efficiency η is defined by the ratio between the number of neutrons N_n produced to the number of incident deuterons N_d; $\eta = N_n/N_d$. Then, η is expressed as

$$\eta = \frac{N_n}{N_d} = N_{Be}\frac{d\sigma}{d\Omega}(\Theta = 0°)\Delta\Omega \tag{7}$$

,

where $N_{Be}(cm^{-2})$ is the areal number density of beryllium nuclei in the target, and $\Delta\Omega$ is the solid angle of the neutron collimator. In our setup, $\Delta\Omega$ was 50 μ sr., so the production angle was assumed to be $\Theta = 0°$. The production efficiencies at the neutron momenta used in the present experiment are shown in Table 3.

****** Table 3 *******

7.1.3 Evaluation of the neutron detection efficiency

The detection efficiency of the neutron beam monitor, ϵ, is given by the following formula which includes neutron production efficiency η :

$$\epsilon = \frac{N_{BM} \cdot \alpha \cdot \beta}{N_{SEC} \cdot \eta} \tag{8}$$

where N_{BM} is the counting rate ($spill^{-1}$) of the "neutral logic" trigger of the neutron beam monitor ($N_{BM} = [\overline{CB} \cdot \overline{F1} \cdot F2 \cdot F3]$), and N_{SEC} ($spill^{-1}$) is the intensity of the deuteron beam measured with the SEC. The neutrons detected in the beam monitor originate not only in the Be target, but also in other materials. α is the correction factor which accounts for neutral particles which do not originate in the Be target. The value of α was determined to be 0.80 ± 0.11 from an analysis of the measured monitor counting rates for various thickness of the Be target.

β is the correction factor to eliminate the gamma contamination in the beam. The amount of the gamma contamination was evaluated in the following way by a measurement with 2 mm thick lead plate ($0.36X_0$) installed in front of the neutron beam monitor. The lead plate increased the "charged trigger" counting rate by Δc , which is expressed as

$$\Delta c = C_n \cdot n + C_\gamma \cdot g \tag{9}$$

where C_n and C_γ are the production efficiencies of charged particles in the lead plate by a neutron and a gamma, respectively, n ($spill^{-1}$) and g ($spill^{-1}$) are the amount of neutrons and gammas, respectively, in the beam. While, the "neutral trigger" counting rate without the lead plate is expressed as

$$N = D_n \cdot n + D_\gamma \cdot g \tag{10}$$

where D_n and D_γ are detection efficiencies for neutrons and gammas, respectively. The production and detection efficiencies were evaluated by a Monte Carlo simulation. For the gammas in the beam, however, as the energy band would be quite wide, the evaluation was performed for the energy from 2 MeV to 3 GeV. Using the values of Δc and N obtained in the measurement, we derived the n and g from the equations (9) and (10) to determine β defined as $\beta = n/(n+g)$. The value of β evaluated at 3 GeV was 0.94 ± 0.07, and the error was dominated by uncertainties in the determination of the C_n and C_γ due to unknown energy spectrum for gammas. As the measurement was carried out only at the neutron beam energy of 3 GeV due to limited machine time, we used the same β for the analyses at the different energies.

The estimates for the neutron detection efficiencies at the momenta studied in this experiment are summarized in Table 4 along with the source of the error in Table 5. Note that they were comparable to the expected value of 1.26 %, calculated from the total thickness of the plastic scintillator(1.0 cm) and the known nuclear interaction length [13].

********* Table 4 **********

******** Table 5 **********

7.2 Monte Carlo simulation of the neutron detection efficiency

As another estimation of the detection efficiency of the neutron beam monitor, we performed a Monte Carlo simulation using the GEANT 3.15 code in the CERN Program Library [14] . The GEANT program can accommodate three generator codes, TATINA [2] , GHEISHA [3], and FLUKA [4] for hadronic interactions. Since FLUKA is the most recently developed code and has the ability to deal with neutron reactions from 50 MeV to the TeV region [14] [15], it is most useful for our purpose. However, the simulation was performed with each generator code to allow a comparison of the sensitivity. The simulation determined the energy deposited in each plastic scintillator bar. Comparing the energy deposited to the threshold of the discriminator, the trigger condition was judged. In the measured pulse-height spectra the energy scale was calibrated with the minimum ionization peak obtained with the "charged logic" trigger. In the simulation the most significant fluctuation of the trigger condition was due to the energy resolution near the threshold, which was measured to be 35% at 2 MeV in our detector spectra. The events were carefully generated taking account of the actual energy resolution. The influence due to the finite resolution on the detection efficiency was, however, small; $\Delta\epsilon/\epsilon = 2 \sim 3\%$ for a change in the resolution from 25 − 35% . The results of the simulation are shown in Table 6 and plotted in Fig.6 for the three generator codes, along with the efficiencies as measured with deuteron beam. As one can see in Fig.6, difference among the generators was found to be at most $\sim 20\%$. However, it is notable that the results of the two different methods, one from the deuteron intensity and another from the simulation, agree well within the errors of the latter method in the region of neutron energies larger than 2 GeV. The detection efficiency at 1 GeV obtained from the measured rates is slightly larger than predicted in the simulations. A possible reason for the discrepancy is the following. The nucleon-nucleon interaction cross section near 1 GeV depends strongly on the incident energy; the cross section increases rapidly as the incident energy increases because the threshold of the Δ resonance is located in this region. This could produce some difficulty in the simulation, and in the evaluation of the neutron flux from the known deuteron beam intensity since this method is based on an interpolation of few measured values of neutron production cross section in this energy region.

****** Table 6 *******

8 Summary

We have constructed a neutron beam monitor to measure the profile and flux of a neutron beam in the few GeV region at the KEK-PS. It has provided useful information about the condition of the neutron beam for the experiment E235 at KEK. The detection efficiency was estimated using two methods : one from the intensity measurement of the deuteron beam, the other from a Monte Carlo simulation. Both methods give consistent results at neutron energies from 2-3 GeV.

9 Acknowledgement

We would like thank the KEK-PS machine crew for their skilful machine operation, the beam channel group for construction of the neutron beam line, and the radiation safety control group for their useful advice. We are pleased to acknowledge the help of Mr. M.Nakagawa and Mr. T.Yamashita. The authors from Nagoya University wish to acknowledge the advice and the support of Dr. K.Kageya, Dr. N.Hayashi, Mr. A.Kishi, Mr. T.Yamada, Mr. S.Toyoda and Mr. T.Ohta. We are indebted to Professors K.Nakai and T.Ohshima for their assistance in performing this experiment.

References

[1] W.B.Amian et al., Nucl. Instrum. and Meth. A281 (1989) 353
R.C.Byrd et al., Nucl. Instrum. and Meth. A313 (1992) 437
S.Albergo et.al., Nucl. Instrum. and Meth. A311 (1992) 280
Th.Blaich et al., Nucl. Instrum. and Meth. A314 (1992) 136
S.Bhadra et al., DESY preprint 94-084

[2] A.Baroncelli, Nucl.Instrum. and Meth. 118, 448 (1974)

[3] H.C.Fesefeldt. Simulation of hadronic showers, physics and applications. Technical Report PI-THA 85-02, III Physikalisches Institut, RWTH Aachen Physikzentrum, 5100 Aachen, Germany, September 1985.

[4] P.A.Aanic et al., Fluka user's guide. Technical Report TIS-RP-190, CERN, 1987, 1990.

[5] H.Noumi et al., Proceedings of the 9th Symposium on Accelerator Science and Technology(August.1993) p.205-207.

[6] M.A.Kovash et al.,KEK-PS Proposal E235.(October,1990).

[7] M.Numajiri et al., The 9th Symposium on Accelerator Science and Technology, Tsukuba, Japan 1993, p428 M.Ieiri et al., The 9th Symposium on Accelerator Science and Technology, Tsukuba, Japan 1993, p477.

[8] J.Banaigs et al., Nucl. Instrum. and Meth., 95,307(1971)

[9] K.Kozma and J.Kliman, J.Phys.G, Nucl. Part. Phys. 16, 45 (1990)

[10] Richard L.Lander et al., Nucl. Instrum. and Meth. III (1973) 445

[11] G.Bizard et al., Phys.Rev. 137, B1228 (1965)

[12] Bevalac Users Manual, pp.II-8

[13] Particle Data Group, Phys.Lett. B204(1988)

[14] F.Carminati et al., GEANT User Guide, Program W5013.CERN, 1993

[15] A.Fasso et al., Nucl. Instrum. and Meth., A332 (1993) 459

Table 1 : The dead time correction. m and n are "measured" and "true" counting rate, respectively. τ is the dead time.

Logic	m(/spill)	m τ (msec)	corr. factor	n(/spill)
CB	2.97×10^5	13.4	1.03	3.06×10^5
F1	5.54×10^5	13.8	1.03	5.72×10^5
F2	6.89×10^5	13.8	1.03	7.10×10^5
F3	1.00×10^6	23.1	1.05	1.06×10^6
$\overline{CB} \cdot \overline{F1} \cdot F2 \cdot F3$	3.41×10^5	6.82	1.02	3.46×10^5
$\overline{F1} \cdot F2 \cdot F3$	3.55×10^5	7.10	1.02	3.61×10^5
$F1 \cdot F2 \cdot F3$	2.07×10^5	4.13	1.01	2.09×10^5
$\overline{F1} \cdot F2$	4.64×10^5	9.27	1.02	4.74×10^5

Table 2 : The accidental coincidence correction.

Logic	corr. factor	corrected (/spill)
$\overline{CB} \cdot \overline{F1} \cdot F2 \cdot F3$	0.99	3.427×10^5
$\overline{F1} \cdot F2 \cdot F3$	0.99	3.577×10^5
$F1 \cdot F2 \cdot F3$	0.995	2.083×10^5

Table3 : Production efficiency from deuteron to neutron beams as a function of the energy and the momentum of the neutron.

T_n (GeV)	P_n (GeV/c)	production efficiency
1.00	1.70	$(1.16 \pm 0.31) \times 10^{-3}$
2.00	2.79	$(2.14 \pm 0.58) \times 10^{-3}$
2.35	3.15	$(2.46 \pm 0.67) \times 10^{-3}$
2.70	3.52	$(2.79 \pm 0.75) \times 10^{-3}$
3.00	3.83	$(3.07 \pm 0.84) \times 10^{-3}$

Table4 :Estimates of the monitor detection efficiencies for neutrons based on the measured deuteron beam intensities.

T_n (GeV)	P_n (GeV/c)	detection efficiency ϵ (%)
1.00	1.70	1.24 ± 0.41
2.00	2.79	1.03 ± 0.34
2.35	3.15	0.86 ± 0.28
2.70	3.52	0.86 ± 0.28
3.00	3.83	0.83 ± 0.27

Table5 : Source of the error of the monitor detection efficiency.

Source of the error	relative error
SEC calibration	0.11
neutral particles not from Be-target(α)	0.14
gamma contamination (β)	0.07
neutron production efficiency η	0.27
total error	0.33

Table6 : The detection efficiencies obtained by the simulation, along with the values estimated from the measured deuteron beam intensity (I_d).

T_n	P_n	detection efficiency ϵ (%)			
(GeV)	(GeV/c)	FLUKA	GHEISHA	TATINA	from I_d
1.00	1.70	0.85	0.87	0.72	1.24 ± 0.41
2.00	2.79	0.91	0.93	0.84	1.03 ± 0.34
2.35	3.15	0.96	0.93	0.88	0.86 ± 0.28
2.70	3.52	0.93	0.87	0.85	0.86 ± 0.28
3.00	3.83	0.99	0.87	0.85	0.83 ± 0.27

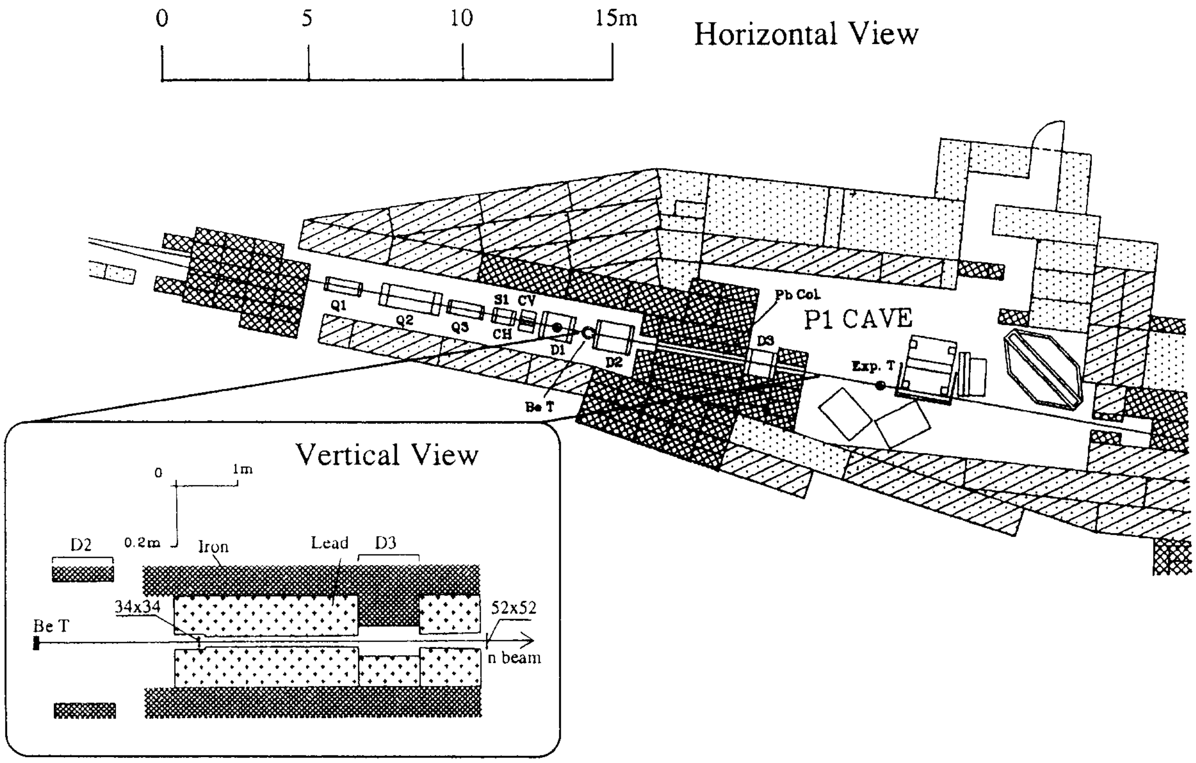

Fig.1: Schematic view of the neutron beam line in the KEK-PS P1 beam channel.

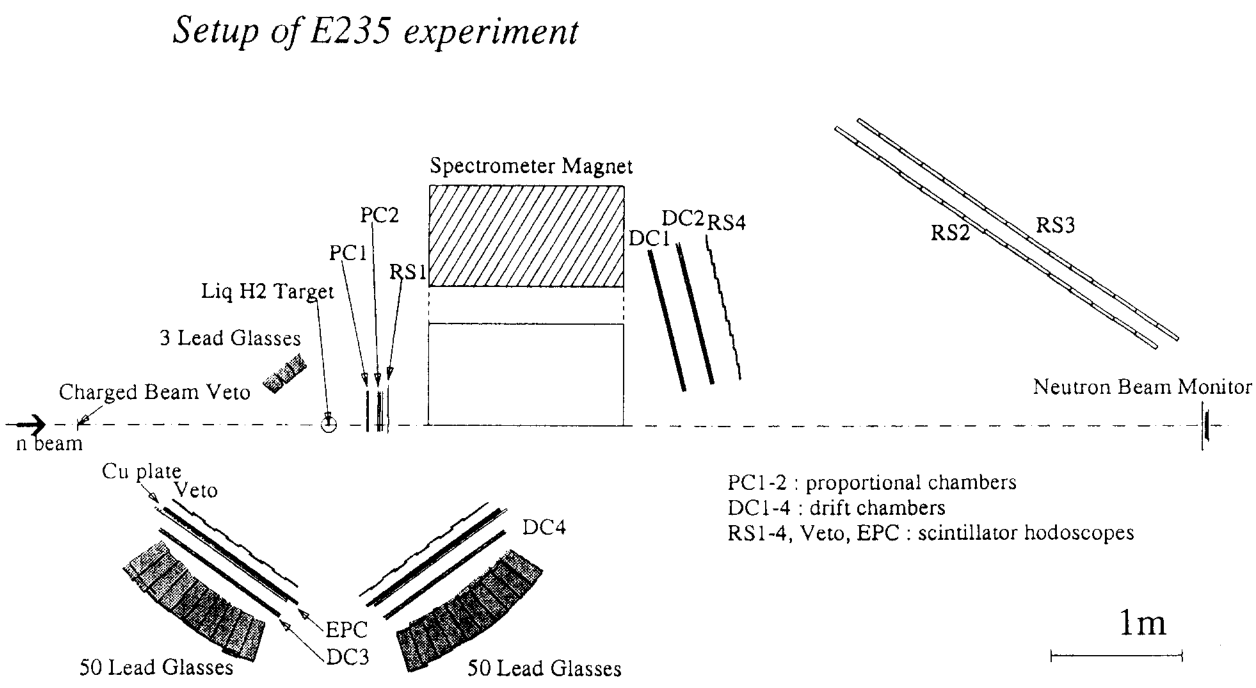

Fig.2: The layout of the experiment E235 at KEK-PS; n+p $\rightarrow$ d+γ differential cross section measurement.

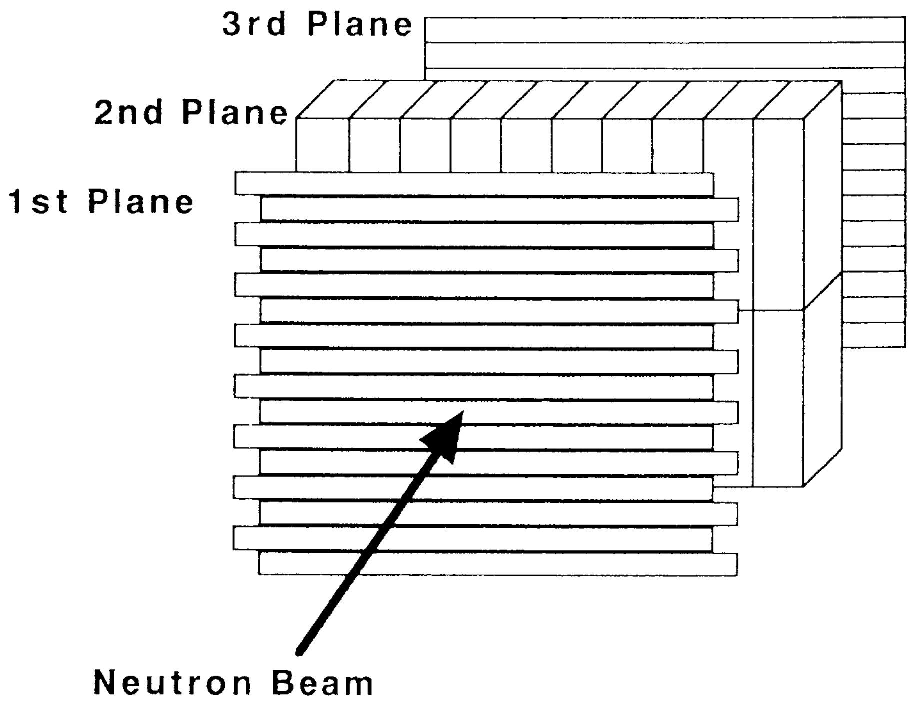

Fig.3: A schematic view of the neutron beam monitor.

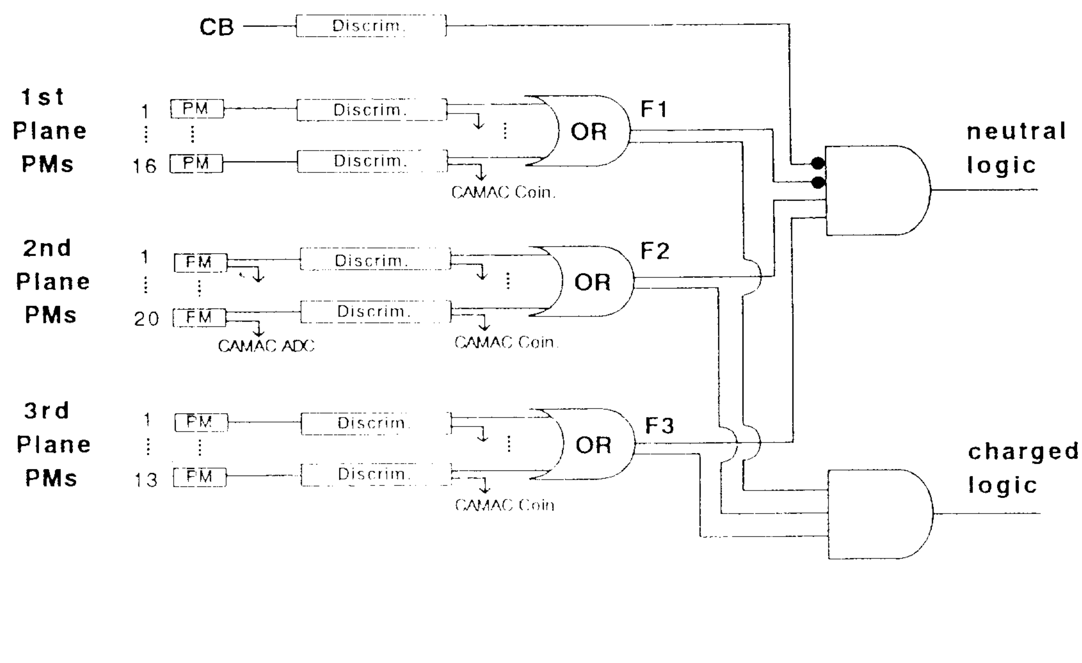

Fig.4: Electronics diagram for the neutron beam monitor.

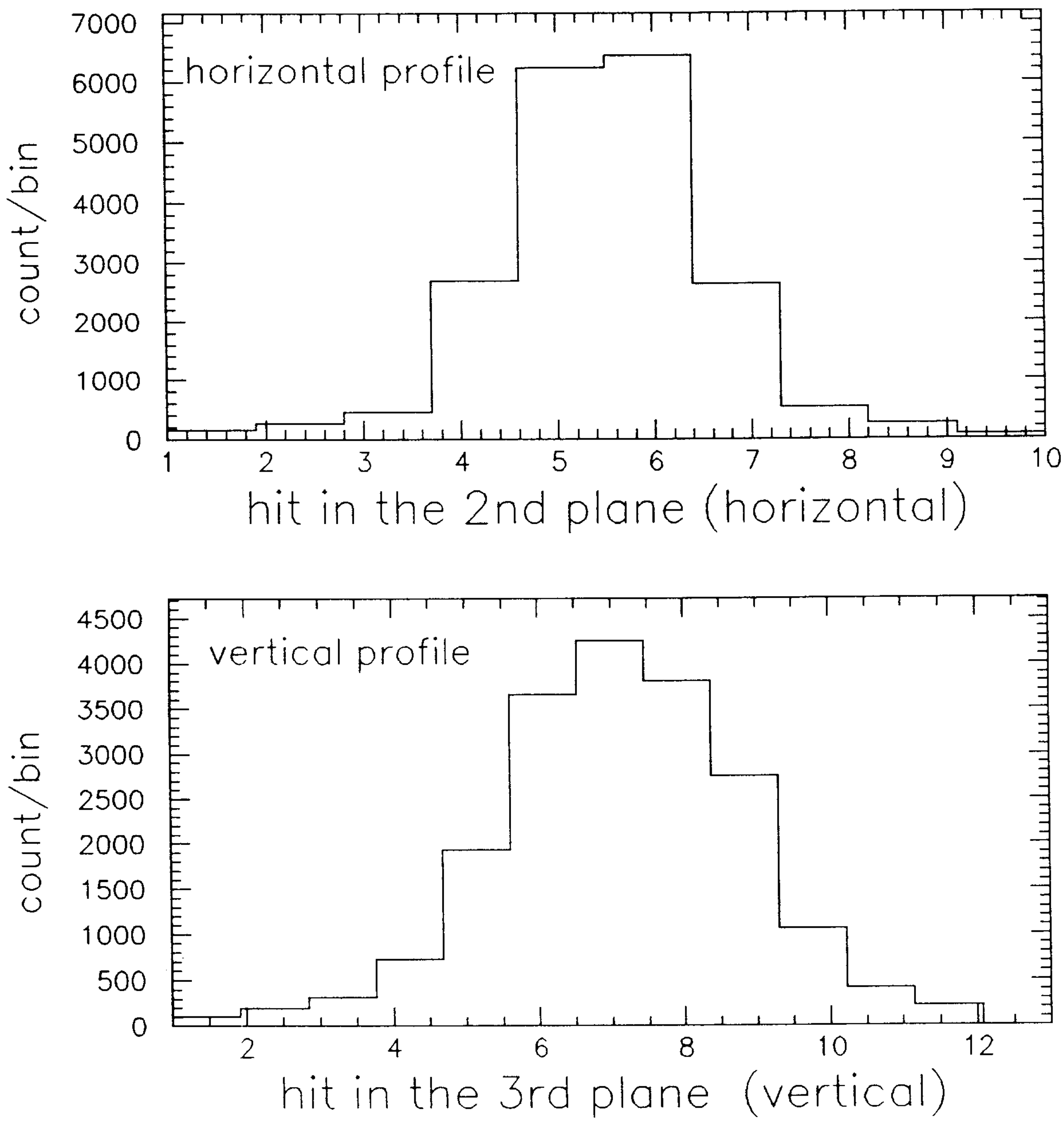

Fig.5: The measured neutron beam profile at the position of the liquid hydrogen target.

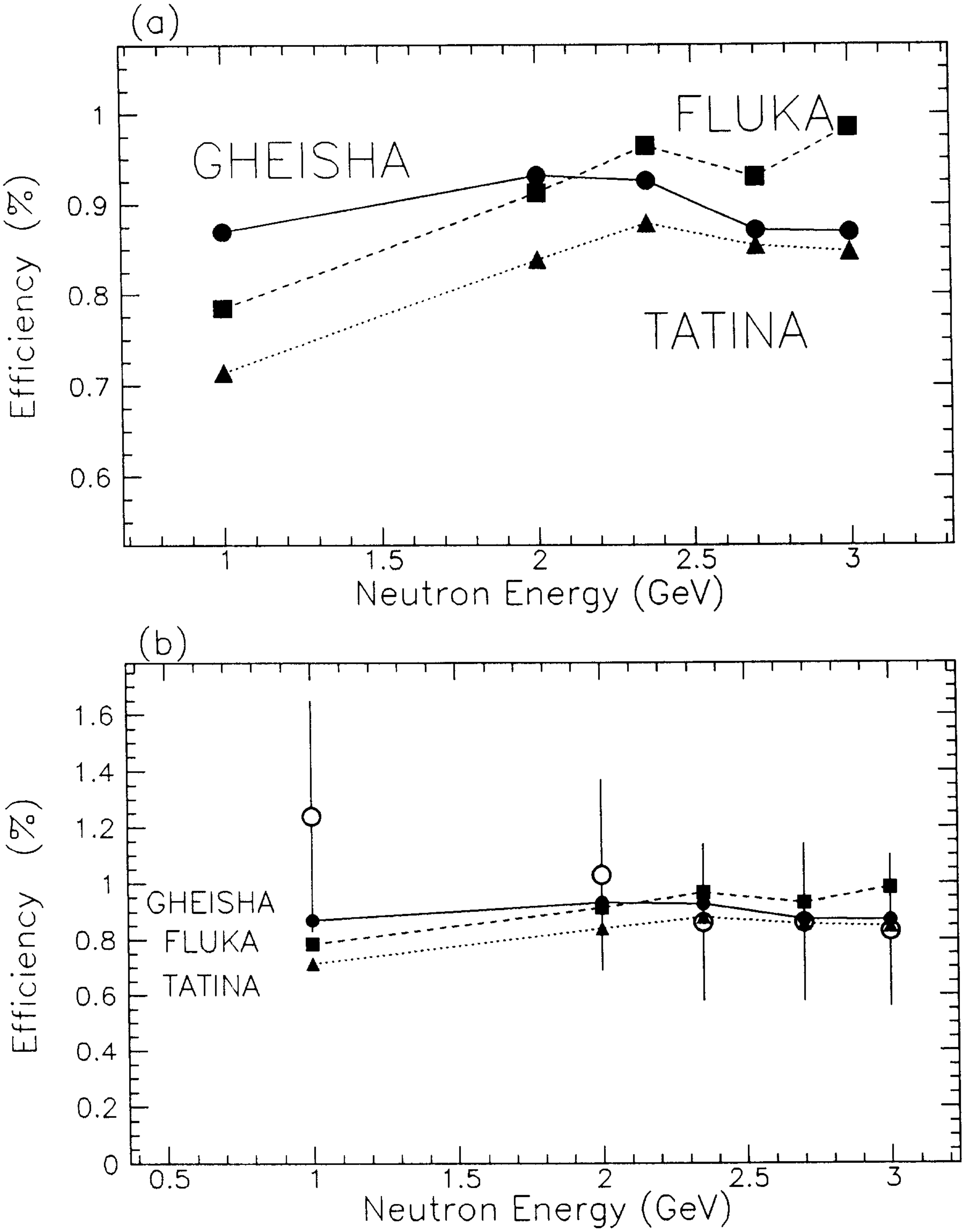

Fig.6: (a) The detection efficiencies obtained with the simulations using three generator codes as a function of the neutron momentum. (b) The same along with detection efficiencies evaluated from the deuteron beam intensity measurement, which are indicated by open circles.